

Airfoil Shape Impact Assessment for Improved Aerodynamics in Hybrid VAWT Applications

Muhammad Ahmad*, Muhammad Zubair Abid

Department of Aerospace Engineering, College of Aeronautical Engineering, National University of Sciences and Technology, Islamabad 4400, Pakistan

*Corresponding author: Muhammad Ahmad, muhammad.ahmad@cae.nust.edu.pk

Copyright: © 2023 Author(s). This is an open-access article distributed under the terms of the Creative Commons Attribution License (CC BY 4.0), permitting distribution and reproduction in any medium, provided the original work is cited.

Abstract: Efficient energy harnessing from renewable energy sources such as wind has gained significant importance in the quest for sustainable power generation. This study focuses on investigating the pivotal role of airfoil shape variations in augmenting the aerodynamic performance of a hybrid vertical axis wind turbine (VAWT). The performance metrics under scrutiny encompass the power coefficient and torque, crucial indicators of a turbine's energy conversion capabilities. In the pursuit of enhancing turbine efficiency, an array of airfoil profiles was curated for evaluation. The selection of an optimal airfoil played a paramount role in shaping the initial investigation. The chosen airfoil, incorporated with a distinctive J-shaped configuration, was subjected to comprehensive analysis within the context of the hybrid VAWT design. The study delves into the intricate interplay between airfoil design and performance parameters. Of particular interest is the power coefficient, where notable advancements were observed. A peak power coefficient of 0.24 at a tip speed ratio (TSR) of 1.25. The investigation yielded a remarkable peak power output of 526 watts, achieved at a rotational speed of 26 revolutions per minute (RPM). Furthermore, a comparative analysis of computational fluid dynamics (CFD) and experimental results in terms of power coefficient (C_p) versus TSR was conducted, revealing a maximum percentage difference of 4.8%. This achievement underscores the tangible impact of

the J-shaped configuration on the turbine's energy conversion capabilities. The consequential increase in power output holds significant implications for enhancing the energy yield of the Hybrid VAWT in real-world applications.

Keywords: Airfoil; Aerodynamics; Hybrid VAWT; Torque; Power efficient

1. INTRODUCTION

In recent times, the energy crisis has significantly intensified, to the extent that the accessibility of electricity has become a commodity restricted to a select few. The energy challenge extends beyond urban areas and impacts those living in remote, off-grid regions where establishing a nearby power plant is not feasible. In the absence of a stable and established power infrastructure, residents are compelled to take matters into their own hands, resorting to generator installations and embarking on demanding and sometimes lengthy journeys to procure fuel supplies. Additionally, the scarcity of fuel renders such methods of electricity generation unsuitable for long-term planning and sustainability [1]. Moreover, the number of increasing natural disasters over the last few years has severely damaged the infrastructure of many nations leading to thousands of people being deprived of power. Considering the magnitude of storms, the process of rebuilding electrical grids progresses at a

sluggish pace, potentially spanning several years. This delay adversely affects the well-being of both the affected populace and the region, hampering their recovery efforts. For instance, in 2017, Hurricane Maria wreaked havoc on Puerto Rico's electrical grid, leading to a total blackout for the population. Even after three months, half of the population still lacked access to electricity, and projections indicated that certain areas might remain without power for up to eight months [2].

1.1. RENEWABLE ENERGY

Renewable energy encompasses naturally occurring sources like solar and wind energy, distinct from nuclear or fossil fuels. This field is rapidly expanding in response to the growing demand for cost-effective and environmentally friendly power alternatives [3,4]. Among these innovations, wind energy harnessed through wind turbines is prominent. Wind power is a notable energy source, achieved by converting mechanical energy from rotating blades, which can be oriented along horizontal or vertical axes. In the United States, wind energy contributes to 5.6% of the total annual energy production, establishing itself as the second most significant renewable energy source, following hydropower [1,5].

1.2. OFFSHORE VERSUS ONSHORE WIND ENERGY

Offshore and onshore wind energy represent two distinct but complementary facets of harnessing wind power for electricity generation. Onshore wind farms are situated on land and are more common due to their lower installation costs. They are well-integrated into existing power grids and infrastructure. In contrast, offshore wind farms are located in bodies of water, often in deeper offshore areas, and offer several advantages, including stronger and more consistent winds. However, offshore installations are typically more expensive and logistically challenging. Both onshore and offshore wind energy play essential roles in the transition to clean and sustainable energy sources, each with its unique set of benefits and considerations [6,7].

1.2.1. CHARACTERISTICS OF ONSHORE WIND ENERGY

Onshore wind energy is characterized by its cost-

effectiveness and ease of integration into existing power grids, making it a widely adopted renewable energy source. Its reliability and consistent energy production are key attributes of harnessing the power of wind on land. A few characteristics of onshore wind energy are given below:

- Typically, wind turbines are situated in regions characterized by low conservation and habitat values.
- Since these are located closer to the electricity consumers, the loss of voltage through transmission lines is considerably less.
- The cost of installing such a turbine is also lower in comparison due to its closer proximity, resulting in reduced transportation expenses.
- Due to its proven technology, these turbines undergo less wear and tear thus reducing the maintenance costs.
- On the downside these turbines if present in the form of large-scale farms can be a source of severe noise pollution if located near populated areas.
- Furthermore, onshore winds are not consistent, with sudden gusts along with long periods of still air conditions. Wind directions are continuously changing reducing the efficiency of wind turbines [8].

1.2.2. CHARACTERISTICS OF OFFSHORE WIND ENERGY

Offshore wind energy is characterized by its potential for harnessing stronger and more consistent winds, resulting in higher energy production compared to onshore counterparts. Additionally, it minimizes land use conflicts and offers the advantage of larger and more efficient turbines for sustainable power generation [9,10]. A few characteristics of offshore wind energy are presented below:

- Offshore wind turbines are strategically positioned in aquatic environments to capitalize on the enhanced wind speeds prevalent in these areas, significantly boosting their power generation capabilities. Furthermore, these regions provide consistent wind speeds and directions, leading to improved turbine efficiency.
- Due to a large and complex setup, the resulting

costs are also significantly high making the choice of HAWT capital-intensive.

- Once the facility is built, ongoing maintenance becomes essential, primarily due to the facilities' oceanic location, which exposes them to higher levels of corrosion and wear. These factors contribute to the already substantial initial installation costs.
- Since the parts have to be transported out to the water bodies, both land and sea costs are invoked.
- The problem of noise pollution is basically non-existent in the case of offshore wind turbines.
- Offshore wind turbines do not take up any land thus more can be allocated to other means like increasing agricultural land or expanding an urban zone.
- Offshore wind farms have the potential to provide benefits to marine ecosystems. Research suggests that these wind farms can contribute to the protection of sea life by limiting access to specific areas and creating additional artificial habitats [11,12].

1.3. TYPES OF WIND TURBINES

Wind turbines are commonly categorized into two primary types:

- Horizontal axis wind turbine (HAWT)
- Vertical axis wind turbine (VAWT)

The HAWT is characterized by its three blades, which are positioned upwind of a tower. HAWTs are responsible for generating a major chunk of the world's wind power. They are typically large installations that require ample space and are most efficient when clustered together as wind farms [13].

A comparison between the properties of HAWT and VAWT is shown in **Table 1**. These include typical values of torque, tip speed ratio (TSR), cut-in speed, and power coefficient. The following comparisons can be made:

- The HAWT operates at higher TSRs (typically around 6) compared to a VAWT.
- The HAWT generates relatively low torque values at higher RPM. On the other hand, the VAWT performs more effectively at lower RPM, producing higher torque.
- The cut-in speed, which is the minimum wind

speed required for a wind turbine to start generating power, is typically higher for HAWTs compared to VAWTs.

- The power output of HAWTs is generally higher than that of VAWTs. HAWTs have been found to be more efficient in converting wind energy into electrical power, resulting in overall more power output.
- The incorporation of a yawing system adds complexity to the design of a HAWT. This mechanism allows the turbine to align itself with the wind direction for optimal performance. In contrast, a VAWT does not require a yawing system as it is inherently omnidirectional and can capture wind from any direction.

Vertical axis wind turbines are typically classified into several distinct types, each with its unique design and operational characteristics:

Darrieus wind turbine: These turbines, often known as Lift-based turbines, typically exhibit a distinctive eggbeater-like appearance. However, variations in the airfoil blade configurations used in Darrieus Wind Turbines can result in different shapes, including the helical design, referred to as Helical Turbines. It is worth noting that the Darrieus model has a notable drawback – the occurrence of a significant torque ripple effect. This effect can lead to increased mechanical stresses and reduced reliability, especially in the H-type turbine variant. Additionally, these turbines usually require an external power source to initiate rotation due to their relatively low starting torque [15,16].

Table 1. Comparative analysis of salient features of HAWT and VAWT [14]

Characteristics	HAWT	VAWT
TSR	6	1 to 3
Torque	Low	High
RPM	High	Low
Cut-in speed (m/s)	5	2 to 5
Power coefficient	0.40	0.15 to 0.40
Yawing mechanism	Required	Not required

The Darrieus wind turbine operates on the principle that, when its blades rotate at a speed greater than the incoming upstream velocity, they generate lift due to the apparent wind created. However, this reliance on apparent wind velocity renders the Darrieus wind turbine non-self-starting, representing a significant drawback. Despite this limitation, the Darrieus wind turbine boasts several promising features that make it a compelling choice among VAWTs. One key advantage of VAWTs, including the Darrieus design, is their symmetrical blade configuration. This symmetry eliminates the requirement for precise wind alignment and negates the need for costly yaw systems, simplifying their operation and reducing overall maintenance costs [17]. Furthermore, VAWTs offer the advantage of having blades attached both at the top and bottom, subjecting them primarily to tensile loading. Consequently, there's no need for blade tapering, simplifying manufacturing processes and rendering blade production cost-effective with reduced fatigue concerns. Moreover, the eggbeater design characteristic of the Darrieus wind turbine incorporates airfoil sections across each blade segment, each oriented at a unique angle of attack. This distinctive design empowers the turbine to autonomously regulate and maintain the necessary rotational speed, contributing to its operational efficiency [14,18].

The original Darrieus wind turbine featured symmetrical airfoils composed of NACA0015 and NACA0018 profiles. This selection was initially motivated by the idea that it would generate maximum lift consistently on both sides of the surface. However, the frequent transitions between negative and positive angles of attack resulted in undesirable vibrational stresses and significant noise emissions [19,20].

Savonius wind turbine: These turbines are also referred to as drag-type turbines and have the significant ability to self-start. The Savonius wind turbine is commonly employed on the rooftop and has adaptations for utilization on ships. These turbines consist of two oppositely curved surfaces. By overlapping the blades near the axis of rotation, the Savonius wind turbine can generate additional torque from the aerodynamic forces. These drag force-dependent turbines rotate their blades at low TSRs, typically not exceeding 1.0 to 1.4 which implies that the turbine would still be able to generate power even at low rotational velocity. The Savonius wind turbine achieves its highest efficiency

within the range of TSRs from 0.4 to 0.7, exhibiting a performance coefficient of 0.15. Savonius wind turbines offer several significant advantages, including self-starting capability, low cut-in speed, absence of a yawing mechanism requirement, compact physical footprint, and straightforward construction [21–23].

Hybrid wind turbine: A hybrid wind turbine combines the characteristics of the Darrieus and Savonius wind turbines, integrating the respective advantages of both types. The goal of hybrid wind turbine was to harness the high starting torque, improved efficiency, and power production capabilities of the Darrieus turbine, along with the self-starting capability of the Savonius turbine. An example of a hybrid design is the Ropatec WRE.060 model, which has the features of two asymmetrical airfoils. The hybrid wind turbine possesses a cut-in speed of 2 m/s and can achieve optimal speeds of up to 14 m/s. The Ropatec turbine also includes a braking mechanism, causing it to stall at higher velocities, typically above 63 m/s. Other examples of hybrid VAWTs include helical and turby wind turbines.

In a recent study, the significant advancements in VAWT technology over the past few decades were examined. The study conducted a thorough analysis of the impacts of different design parameters, such as airfoil shape, blade count, solidity, aspect ratio, blade helicity, and overlap ratio. The research revealed that fixed-blade Darrieus turbines face challenges in initiating rotation at low wind speeds, whereas Savonius turbines exhibit favorable starting capabilities with lower power coefficients compared to alternative types of VAWTs. To overcome the limitations of traditional wind turbines, engineers pursued innovative solutions by developing hybrid VAWTs through advanced designs. The analysis indicated that hybrid wind turbines have made some progress in addressing these limitations, although their overall performance still lags behind that of conventional wind turbines [24–26].

When comparing lift-based that is Darrieus and drag-based that is Savonius VAWTs, it is observed that lift-based turbines have higher power coefficients than their drag-based counterparts. Nevertheless, lift-based turbines have a disadvantage in terms of low starting torque, rendering them incapable of self-starting at low wind speeds. In contrast, drag-based turbines demonstrate favorable self-starting capabilities. Hybrid VAWTs

encounter specific challenges, including the requirement for design optimization of a more intricate system, concerns related to vortex shedding, and relatively lower performance at high TSR values due to the drag forces produced by the Savonius turbine [27,28]. However, modified hybrid VAWTs can overcome the limitations of conventional VAWTs, including achieving a high C_p at a wider range of TSR and self-starting characteristics. Several investigations have been conducted to enhance the self-starting capability, primary torque, and operational range of hybrid VAWTs. The objective is to explore different design configurations to achieve optimal design and performance parameters [2,29].

In recent times, there has been a growing interest among researchers in both academic and industrial sectors regarding the implementation of VAWTs. These turbines possess the significant advantage of being able to harness wind energy from any direction. This capability becomes particularly advantageous in urban areas where wind conditions are highly variable, with changing wind direction and varying magnitudes, often accompanied by sudden gusts. Urban environments are characterized by numerous obstacles such as tall buildings that obstruct or even completely block airflow. Therefore, the ability of VAWTs to capture wind from multiple directions makes them a promising solution for harnessing wind energy in urban settings. The idea of the VAWT has been incorporated in many urban areas by utilizing rooftops of tall construction buildings to provide a clean source of energy to the neighboring residential areas [30].

The characteristics of three configurations of VAWT are presented in **Table 2**. These include the number of blades, TSR, power coefficient, and self-starting abilities. The summary of the comparative analysis is as follows:

- The hybrid wind turbine requires more blades because it is a combination of both Darrieus and Savonius designs.
- The Darrieus turbine functions at relatively higher values of TSR ranging from 1–3 than the Savonius design which operates between 0.4 to 0.7.
- Under identical input conditions, the Darrieus wind turbine outperforms the Savonius wind turbine in terms of power generation.
- The Savonius wind turbine possesses a notable

self-starting capability than the Darrieus wind turbine. However, the hybrid wind turbine combines the advantages of both turbines, including incorporating the self-starting ability of the Savonius wind turbine.

Based on the data presented in **Table 2**, it is evident that the Savonius wind turbine, while self-starting and straightforward to build, may not be the ideal choice for constructing a small-scale VAWT model due to its notably low TSR values. Given this discussion, it is anticipated that the Savonius model may not yield sufficient electricity generation. Conversely, the Darrieus wind turbine emerges as a promising candidate, primarily owing to its potential for delivering higher efficiencies. The curvature of its blades ensures operation at optimal TSRs, even when wind speeds exceed the ideal values. However, a significant drawback lies in its lack of self-starting capabilities. Furthermore, achieving the required blade curvature to form the airfoil profile for the Darrieus design poses complexity, coupled with challenges in sourcing the necessary materials. Consequently, this makes it an unsuitable choice for the construction of a small-scale prototype model [31]. After assessing both the Darrieus and Savonius turbines, the hybrid design emerges as a promising amalgamation of their strengths. Hybrid configurations offer the best of both worlds: self-starting capability akin to the Savonius design and the ability to operate at higher TSRs, thereby achieving efficiency levels comparable to the Darrieus turbine. Furthermore, hybrid designs exhibit another notable advantage by incorporating a greater number of blades than the Savonius and Darrieus designs. This increased blade count enhances the turbine's stability. Moreover, the unique design of the hybrid VAWT ensures a gradual

Table 2. Characteristics of three different configurations of VAWT [14]

Characteristics	Darrieus	Savonius	Hybrid
Number of blades	2–3	2	3–4
TSR	2–4	0.4–0.7	1–3
Power coefficient	0.3–0.4	0.15	0.20–0.35
Self-start	No	Yes	Yes

and smooth transition between positive and negative angles of attack, which reduces vibrational stresses and subsequently minimizes noise during operation [32–34].

1.4. GENERAL ADVANTAGES OF VAWT OVER HAWT

The following advantages make the VAWT a viable source for producing renewable energy [35,36]:

- One of the key attributes of VAWTs is their capacity to harness wind from all directions. This quality proves particularly advantageous in urban settings, where prevailing wind patterns are often unpredictable due to the presence of various obstacles that disrupt airflow. Urban structures like buildings and other constructions create intricate flow patterns, rendering it difficult to ascertain a dominant wind direction. Engineering constructions are crafted with the intention of enduring the loads they are anticipated to support throughout their operational lifespan [37]. The omnidirectional wind capture capability of VAWTs makes them exceptionally well-suited for urban environments, where wind flow is influenced by multiple impediments within the surrounding terrain.
- A unidirectional VAWT operates autonomously, regardless of wind direction, negating the necessity for intricate mechanisms and motors to adjust the rotor's orientation or blade pitch. This streamlined design eliminates the need for complex yawing or pitching systems commonly present in other turbine types.
- VAWTs hold the advantage of being installable beneath existing HAWTs within wind farms. This strategic placement facilitates additional power generation without the necessity for additional land usage. By harnessing the space beneath HAWTs, VAWTs can effectively enhance the energy production capacity of the wind farm, optimizing overall efficiency without the need for additional land resources [38].

1.5. POWER PRODUCTION OF VERTICAL AXIS WIND TURBINE

Research studies have revealed that arranging VAWTs in

a closely packed configuration can yield power output comparable to that of HAWTs while maintaining high-efficiency levels. The proximity of VAWTs in such an arrangement effectively utilizes wind resources and enhances power generation efficiency. These findings suggest that properly arranged VAWTs can serve as a viable alternative to HAWTs in terms of power production efficiency. Although individual VAWTs may produce less power compared to HAWTs, their tightly packed, counter-rotating arrangement leads to significantly greater power densities. This makes VAWTs a highly efficient and productive choice for wind farms, effectively addressing the major challenge of wind energy – land utilization. While modern HAWT farms typically generate around 2-3 watts per square meter, experiments with VAWT farms have demonstrated the potential to achieve a remarkable production of 30 watts per square meter [39].

The research gap addressed in this study concerns the limited exploration of alternative airfoil shapes, particularly the J-shaped configuration, in the context of Hybrid VAWTs. Previous research predominantly focused on tapered or thin-sliced airfoils, overlooking alternative configurations. This study aimed to bridge this research gap by investigating the J-shaped airfoil with a straight-cut modification. This choice allowed for a comprehensive exploration of the significant disparities between this innovative design and traditional baseline airfoils, offering valuable insights into its aerodynamic behavior within Hybrid VAWTs. This unique configuration promises enhanced performance and efficiency, filling a critical knowledge void in renewable energy technology.

1.6. NOVELTY OF RESEARCH

In the present study, the airfoil shape impact on aerodynamic parameters of Hybrid VAWT has been studied. While previous research has predominantly focused on tapered or thin-sliced variations of the baseline airfoil, we recognize that this limited focus may create gaps in our understanding of these flow regimes. To bridge these gaps and contribute novelty to our research, we have adopted a distinct approach by implementing a J-shaped airfoil with a straight-cut modification, diverging from the thin slice or taper configurations. This strategic straight-cut placement

aligns with well-established trends in J-shaped airfoil investigations. By making this selection, we aim to comprehensively investigate the most significant disparities between the baseline and the modified airfoil, thus providing valuable insights into the aerodynamic behavior of this specific configuration. The airfoil used in this study is visually represented in **Figure 1**.

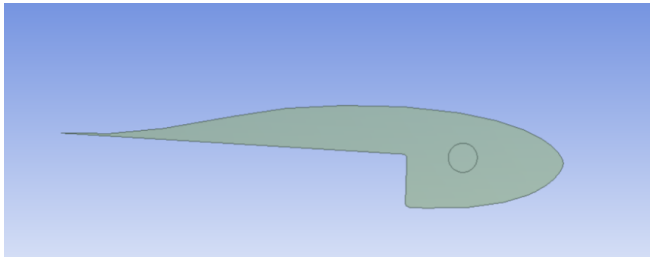


Figure 1. Modified J-shaped airfoil used in hybrid VAWT.

2. THEORETICAL BACKGROUND

2.1. POWER IN WIND

Wind turbines operate by harnessing the energy of incoming air and converting it into kinetic energy, which is subsequently transformed into electricity. This energy conversion process hinges on creating a pressure differential between the front and rear sides of the turbine. As the air moves past the turbine, the rotating blades decelerate the air, inducing a reduction in its pressure. Since air is considered an incompressible fluid at low speeds, this pressure drop occurs just downstream of the turbine. This decline in pressure results from the transfer of kinetic energy from the air to the turbine blades, initiating the rotation of the turbine and ultimately generating electricity. To maintain equilibrium and restore the pressure to atmospheric levels, Bernoulli's principle comes into play, leading to a subsequent increase in air velocity and kinetic energy. This kinetic energy is then harnessed to drive the turbine blades through a system of gears and connections, enabling the production of electricity.

2.2. CUT-IN AND CUT-OUT SPEED

The cut-in speed refers to the wind velocity at which the turbine initiates rotation and subsequently generates electricity. Below this value, the blades cannot rotate and hence no power can be produced. For the case of HAWTs,

a typical value of the cut-in speed is 5 m/s, and in the case of VAWT, the cut-in speed can go as low as 2 m/s. Cut-out speed defines the upper limit for the functional velocity for which the turbine generates electricity. This means that if the oncoming wind has a velocity greater than the cut-off speed then the turbine cannot produce electricity. As the wind velocity increases the blade rotation increases and thus the forces and consequently stresses imparted on the blades, hub, and shaft increase and may result in catastrophic failure of the turbine. Thus, a limiting velocity was defined by the engineers for which the turbine ceases to operate. For general cases, a value of 25 m/s can be selected though safe operations at higher velocities are still achievable [40,41].

2.3. TIP SPEED RATIO

The rotational velocity of a wind turbine plays a crucial role in determining the power generation capacity. In the case of HAWTs, the local velocity vector of the incoming wind is not strongly influenced by the turbine's rotational velocity. However, for VAWTs, the local velocity vector is directly influenced by the rotational velocity of the turbine. To account for these factors, the TSR is commonly used. The TSR is defined as the ratio of the blade tip speed to the upstream velocity of the wind. It takes into consideration the rotational velocity of the turbine blades and their interaction with the incoming wind. By optimizing the TSR, wind turbines can achieve better power generation efficiency, as it helps to match the rotational speed of the blades to the wind speed, thereby maximizing energy extraction from the wind. A higher value of TSR would result in more power production and lower values of torque whereas lower values of TSR would produce a consequent lower power output and higher torque values. For the HAWT typical values of TSR are around 6 while VAWTs operate at lower values of TSR of about 3 however some VAWTs operate at higher TSRs as well.

2.4. AIRFOIL SHAPES

Turbine blades are crafted with a range of airfoil shapes and sizes. The specific shapes of airfoils are selected based on their ability to create a disparity in pressure between the upper and lower surfaces. Due to the shape of the airfoil, the flow over the airfoil surface has to

travel at a higher velocity than that at the bottom surface because the distance that the air particle has to travel is greater at the top surface than at the bottom surface and because the particles must reach the trailing edge at the same time. The start of the airfoil is called the leading edge whereas the end of the airfoil is called the trailing edge. This difference in air particle speeds at the top and bottom surface creates a high-pressure region below the airfoil and a low-pressure region above the airfoil. This difference in pressure results in a net pressure which then gives rise to a force called lift [42,43]. The airfoils in the case of turbine blades are oriented in such a way that they create rotational velocity for the blades rotating them consequently turning the turbine shaft and thus producing electricity. Aircraft wings are generally designed with a thickness ratio of less than 10% because they need to operate at higher velocities and lower angles of attack. However, in the case of turbine blades slower operational speeds and higher angles of attack are available thus they are made of thicker airfoils [44,45].

2.5. VELOCITY AND FORCE VECTORS ACTING ON VAWT

The fundamental equations that are required to construct the mathematical model required to accurately simulate the VAWT are represented in this section. The first thing to take into consideration for a VAWT is that not only the direction of the incoming upstream flow is important but also the direction of the rotation of the turbine blades. This implies that the resultant or local velocity acting on each blade of the VAWT is a resultant of the upstream and the rotational velocity as shown in Equation 1.

$$\vec{W} = \vec{V} + (\vec{\omega} \times \vec{R}) \quad (1)$$

where \vec{W} is the resultant velocity vector, \vec{V} is the incoming freestream velocity, $\vec{\omega}$ is the rotational velocity of the blades and \vec{R} is the rotor radius. This equation implies the local velocity varies during each cycle. The maximum velocity occurs at $\theta = 0$ and the minimum value occurs at $\theta = 180$, where θ represents the azimuth angle.

The angle of attack α is the angle between the oncoming air velocity, \vec{W} , and the blade's chord. From the geometric considerations, it is evident that the tangential component of velocity is as given in Equation 2,

and the normal component is as shown in Equation 3. The resultant of these two velocities gives the local velocity as shown in Equation 4.

$$V_t = \omega R + V \cos \theta \quad (2)$$

$$V_n = V \sin \theta \quad (3)$$

$$W = \sqrt{V_t^2 + V_n^2} \quad (4)$$

Another important factor that can be incorporated into the equation is the tip speed ratio (λ) as presented in Equation 5.

$$\lambda = \frac{\omega R}{V} \quad (5)$$

Encapsulating the TSR into the resultant velocity provides the comprehensive form as shown in Equation 6.

$$W = V \sqrt{1 + 2\lambda \cos \theta + \lambda^2} \quad (6)$$

The angle of attack was determined using the tangential and normal components of the resultant velocity as given in Equation 7.

$$\alpha = \arctan \frac{V_n}{V_t} \quad (7)$$

The forces acting on the VAWT can be categorized either as lift (L), drag (D), normal (N), or tangential (T) force. These forces are normalized based on dynamic pressure to allow for easier comparison of multiple coefficients for different airfoils and to quickly identify the optimal one. The main coefficients are as follows:

- Lift Coefficient (C_L)
- Drag Coefficient (C_D)
- Tangential Force Coefficient (C_T)
- Normal Force Coefficient (C_N)

These coefficients are shown from Equation 8 to 11.

$$C_L = \frac{F_L}{\frac{1}{2} \rho A W^2} \quad (8)$$

$$C_D = \frac{D}{\frac{1}{2} \rho A W^2} \quad (9)$$

$$C_T = \frac{T}{\frac{1}{2} \rho A V^2 R} \quad (10)$$

$$C_N = \frac{N}{\frac{1}{2}\rho AV^2} \quad (11)$$

Power is generated by a VAWT on the mass elevated over the blades. An increase in TSR leads to a decrease in the airflow lifted and thus a consequential decrease in the power output. Other factors that affect the power output are the airfoil and pitch angle [46]. The amount of power that can be produced by the VAWT can be evaluated using Equation 12.

$$P = \frac{1}{2} C_p \rho AV^3 \quad (12)$$

where C_p is the power coefficient, ρ is the fluid density, A is the swept area of the turbine, and V is the wind speed.

2.6. GEOMETRIC PARAMETERS OF VAWT

Table 3 provides an overview of the essential parameters necessary for the construction of a VAWT. It is important to note that this table specifically focuses on the requirements when a single airfoil is chosen for the VAWT design. However, it is crucial to acknowledge that the configuration of the VAWT can be complex, especially when variable airfoil geometry along the chord is employed. In such cases, the properties and considerations of the airfoil may undergo significant changes.

Table 3. Analysis of wind turbine geometry

S No	Parameter	Variable / Fixed
1	Axis of rotation	Fixed
2	Turbine height	Fixed
3	Rotor radius	Fixed
4	Airfoil type	Variable
5	Number of blades	Fixed
6	Swept area	Fixed
7	Cut-in speed	Fixed
8	Cut-out speed	Fixed
9	Wind speed range	Fixed
10	Rotational speed	Variable

3. METHODOLOGY

This section outlines the systematic approach and framework that will guide the project's execution. It serves as a roadmap, delineating the steps, procedures, and overall structure that will be followed to achieve the project's objectives. The framework depicted in **Figure 2** provides a visual representation of this methodological approach, offering a concise overview of the project's workflow and key components.

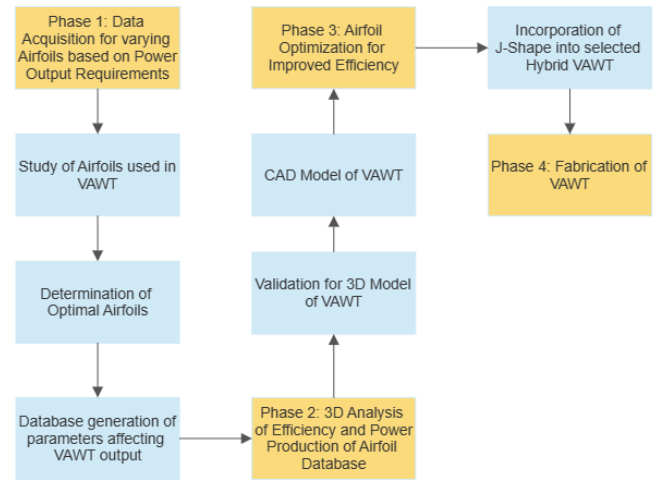


Figure 2. Flow chart showing the methodology adopted during the course of research.

3.1. VALIDATION OF COMPUTATIONAL FLUID DYNAMICS (CFD) MODEL

The validation of a CFD model is a crucial step in ensuring the accuracy and reliability of its predictions. This process involves comparing the model's results with real-world data or experimental measurements to assess its capability to simulate fluid flow and related phenomena accurately [47,48].

3.1.1. GEOMETRY FOR VALIDATION OF CFD MODEL

Table 4 provides a comprehensive compilation of critical dimensions directly associated with the three-dimensional (3D) scenario, offering a quantitative foundation for understanding the spatial intricacies of the system or object under investigation. These dimensions are meticulously documented to facilitate a comprehensive grasp of the 3D environment. Complementing this, **Figure 3** visually illustrates the inner and outer radii

within the inner domain and the dimensions of the outer domain. This graphical representation enhances clarity regarding spatial relationships, making it an invaluable reference for comprehending the geometric characteristics that bear essential significance in the analysis, design, or evaluation of the subject of study.

Table 4. Geometric parameters of VAWT selected for CFD validation [49]

Parameter	Value	Unit
Airfoil	NACA0022	-
Chord length	100	mm
Turbine height	400	mm
Turbine radius	300	mm

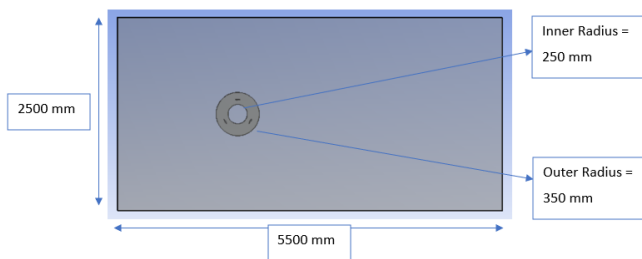


Figure 3. Geometry of VAWT for validation of CFD model.

3.1.2. MESH FOR VALIDATION OF CFD MODEL

The settings outlined in the research paper were replicated for the mesh generation process. To optimize simulation time, a hexahedral mesh was created for the

outer domain. However, this decision led to an increased mesh generation time. For the inner domain, a tetrahedral mesh was generated, and an inflation layer or prism layer was carefully designed near the airfoil surface. This layer was created with consideration for the incoming velocity, growth ratio, and the specified number of layers, ensuring effective near-wall treatment to accurately capture boundary layer phenomena. The generated mesh and associated views are shown in **Figure 4**.

3.1.3. VALIDATION RESULTS FOR MODEL

The initial simulation was conducted at a tip speed ratio of 2.5. Subsequently, a torque plot for the simplified VAWT model was generated, from which the average C_m value was extracted. This average C_m value was then utilized to calculate the corresponding C_p value for the given TSR, as demonstrated in the calculations presented below. Notably, the maximum percentage error observed between the experimental and CFD results was found to be below 6%. These comparative findings are graphically illustrated in **Figure 5**.

3.2. COMPUTER-AIDED DESIGN MODEL FOR HYBRID VAWT

The analysis of the airfoil required a hybrid model of the VAWT, and for this purpose, a suitable turbine model was chosen based on the paper titled “Design optimization of double-Darrieus hybrid vertical axis wind turbine” [24]. The hybrid VAWT used as the baseline model for this analysis is depicted in **Figure 6**. The associated dimensions for the baseline model are shown in **Table 5**.

Further modifications and improvements were made

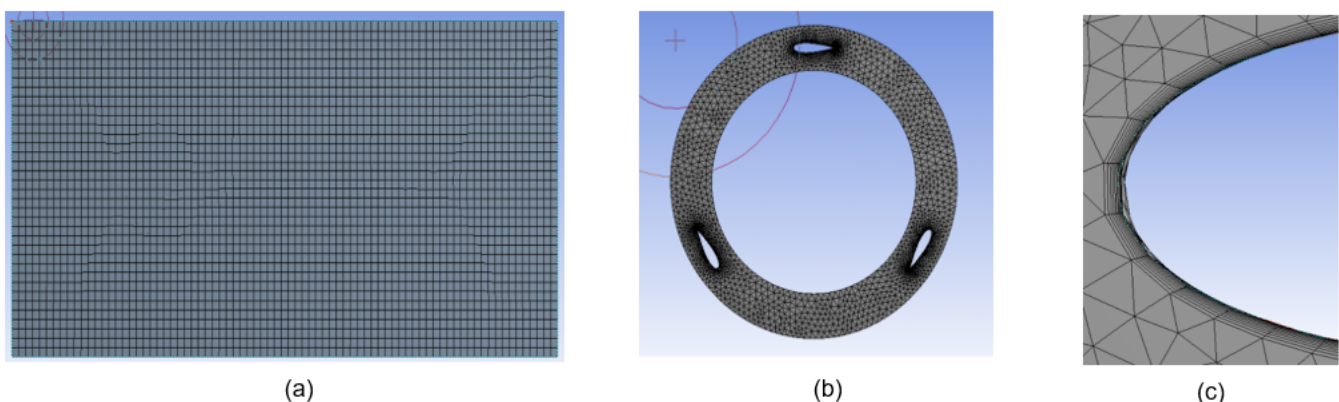


Figure 4. Mesh for validation of CFD model of VAWT. (a) Outer domain; (b) Inner domain; (c) Inflation layer on airfoil surface.

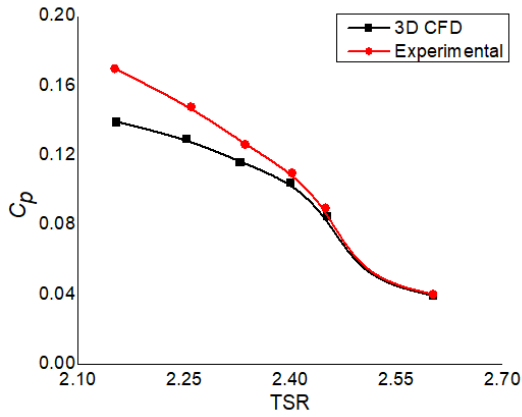


Figure 5. Results obtained for validation of VAWT CFD model.

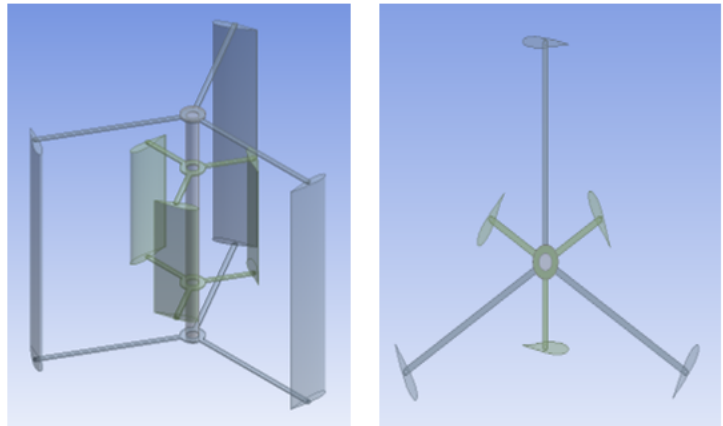


Figure 6. Geometry of baseline hybrid VAWT.

Table 5. Geometric parameters of hybrid VAWT [24]

Parameter	Value	Unit
Outer hub radius	1.927	m
Outer blade chord	0.547	m
Outer blade pitch angle	-2.82	deg
Outer rotor height	3.12	m
Inner turbine radius	0.789	m
Inner turbine chord	0.547	m
Inner blade pitch angle	-3.41	deg
Inner rotor height	1.605	m
Central shaft diameter	0.15	m

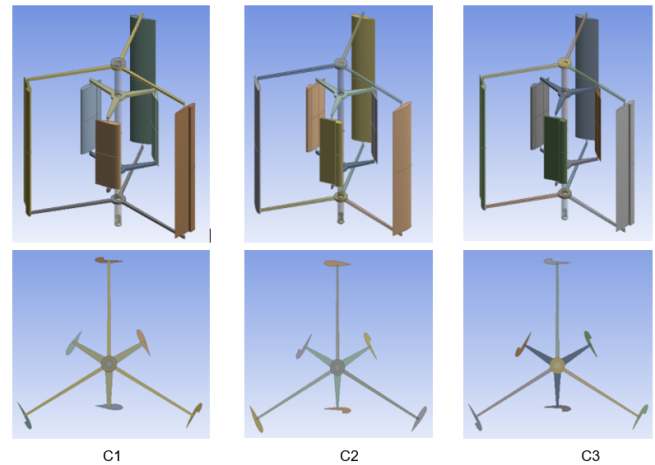


Figure 7. Different configurations of hybrid VAWT.

to this baseline hybrid turbine model. Three distinct configurations were generated: C1, with the J-Shaped airfoil applied to the outer blade; C2, where the J-Shaped airfoil was applied to the inner blade; and C3, featuring the J-Shaped airfoil applied to both the inner and outer blades. These three setups are visually depicted in **Figure 7**.

3.3. GEOMETRY OF HYBRID VAWT

The geometry parameters for both inner and outer domains retained the same settings as those employed previously. Utilizing these settings, the analysis domain for Hybrid VAWT was generated, as illustrated in **Figure**

8. Furthermore, the associated dimensions for the outer domain are presented in **Table 6**.

For the inner domain certain body of influence (BOI) needed to be created near the blade and airfoil trailing edge to ensure better refinement near the blades (refer to **Figure 9**). The associated values selected for this purpose are shown in **Table 7**.

3.4. MESH OF HYBRID VAWT

For meshing the corresponding sizing to each domain entity and BOI was assigned as shown in **Table 8**. The resultant mesh generated is shown in **Figure 10**.

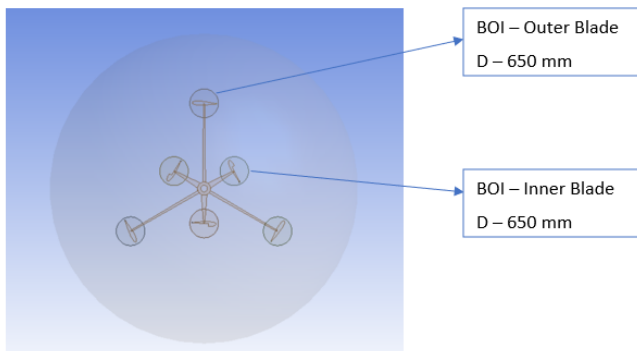


Figure 9. BOI for blades of hybrid VAWT.

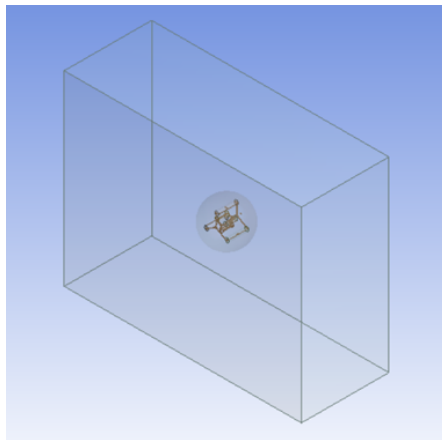


Figure 8. Analysis domain generated for hybrid VAWT.

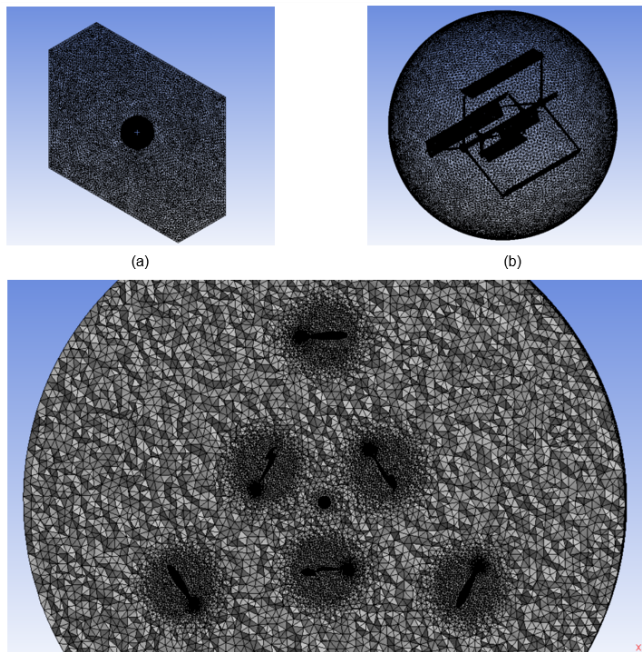


Figure 10. Mesh generated for hybrid VAWT. (a) Isometric view; (b) Inner domain; (c) BOI for inner and outer blades alongside body of influence for inner and outer blade trailing edge.

Table 6. Dimensions of outer domain selected for hybrid VAWT

Parameter	Value	Unit
Domain length	38	m
Domain height	30	m
Domain width	14	m

Table 7. Inner domain sizing for hybrid VAWT

Parameter	Value	Unit
Inner domain radius	3,500	mm
BOI diameter – outer blade	650	mm
BOI diameter – inner blade	650	mm
BOI diameter – outer blade TE	25	mm
BOI diameter – inner blade TE	25	mm

Table 8. Details of meshing parameters for hybrid VAWT

Parameter	Value	Unit
Outer domain sizing	650	mm
Inner domain sizing	100	mm
Shaft and frame sizing	30	mm
BOI – Outer blade sizing	30	mm
BOI – Inner blade sizing	30	mm
BOI – Outer blade TE sizing	4	mm
BOI – Inner blade TE sizing	4	mm

Table 9. Boundary conditions selected to conduct the computational analysis

Boundary condition	Value	Unit
Velocity	7.5	m/s
Outlet	Pressure outlet	-
Top, bottom, and sides	Symmetry	-
Rotational velocity	3.892	rad/s

Table 10. Reference values of the computational domain

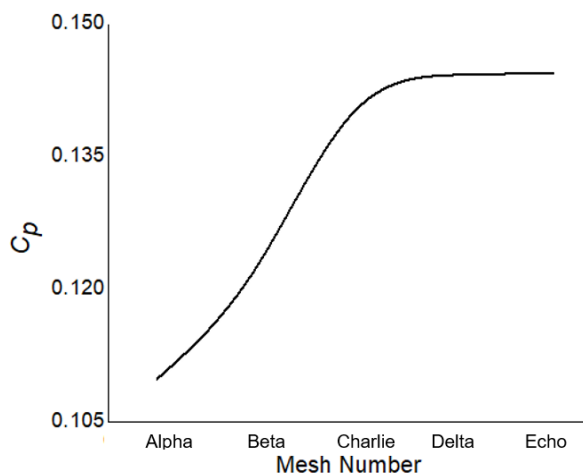
Reference values	Value	Unit
Area	12.02	m ²
Length	0.546	m
Velocity	7.5	m/s

Table 11. Number of time steps and time step size

Calculation inputs	Value
Number of time steps	120
Time step size	0.05 s
Maximum iterations per time step	20

Table 12. Mesh independence study for hybrid VAWT showing inner and outer blade sizing

Mesh name	Element size	Unit
Alpha	70	mm
Beta	50	mm
Charlie	30	mm
Delta	10	mm

**Figure 11.** Mesh independence study for hybrid VAWT.

3.5. CFD SETUP AND SOLVER SETTINGS FOR HYBRID VAWT

To perform numerical simulations, ANSYS software served as the primary tool. This software is renowned for its robust capabilities in CFD analysis, enabling accurate modeling and analysis of fluid flow and heat transfer phenomena in the research. ANSYS's versatile features and user-friendly interface were instrumental in ensuring the reliability and rigor of the numerical simulations. The CFD settings employed within the validation process remained unchanged. Only the inlet velocity, along with the range of TSR applied, underwent modifications. Details about the boundary conditions selected for the computational analysis, the reference values for the computational domain, and the number of time steps and their sizes can be found in **Tables 9–11**.

3.6. MESH INDEPENDENCE STUDY

Mesh independence study for Hybrid VAWT was carried out by varying element sizes as shown in **Table 12**. The Cp value for the hybrid VAWT model was acquired at TSR 1, and the outcomes are depicted in **Figure 11**. Upon analyzing the Cp value, it was determined that Mesh Charlie struck a balance between achieving refined results and minimizing the computational time needed for simulating the hybrid VAWT [50].

3.7. TIME STEP INDEPENDENCE STUDY

Based on the observation, Mesh Charlie was utilized for the time step independence study. The analysis involved variations in the time step size by tenths relative to adjacent values. For example, the initial simulations were conducted at a 0.05 s time step size, and the Cp was evaluated. These simulations were carried out at TSR 1.00 and 7.5 m/s, and the results indicate that a 0.05 s time step size was sufficient to achieve computational efficiency while maintaining reasonable accuracy. The detail of three different time steps chosen for Hybrid VAWT is presented in **Table 13**. The variation of the power coefficient for various time step sizes is presented in **Figure 12** [50,51].

3.8. FABRICATION OF HYBRID VAWT

In the fabrication phase, a 3D printing technique was employed to produce a scaled-down model of the turbine. The dimensions for scaling down the turbine

Table 13. Time step independence study for hybrid VAWT

S No	Time step size	Number of time steps
1	0.5 s	12
2	0.05 s	120
3	0.005 s	1,200

Table 14. Scaling factors for scaled-down hybrid VAWT

Scaling variable	Scaling equation	Scaling factor
Length	S_L	15
Velocity	$S_V = S_L^{0.3}$	2.25
Rotational velocity	$S_\omega = S_L^{-0.5}$	0.26
Mass	$S_M = S_L^3$	3,375
Aerodynamic force	$S_F = S_L^3$	3,375
Power	$S_P = S_L^{3.5}$	13,071.32

were determined based on the limitations imposed by 3D printing technology. These constraints guided the adjustment of dimensions specified in **Table 14**. By adhering to these printing constraints, the selected dimensions ensured compatibility with the 3D printing process. This approach facilitated the creation of an accurate and reduced-scale physical model that faithfully represented the original turbine's design. Aligning the scaled-down dimensions with the printing constraints allowed for the production of a highly detailed model suitable for subsequent experimentation and analysis. A pictorial view of the scaled-down model for C1 and C2 configurations of Hybrid VAWT is shown in **Figure 13**.

4. ANALYSIS AND DISCUSSION

In this section, the analysis of results obtained for performance parameters including C_p versus TSR and power versus RPM for J-shaped Hybrid VAWT configurations is presented. This analysis unveils the impact of TSR variations on the energy conversion efficiency of these configurations, offering valuable insights into their

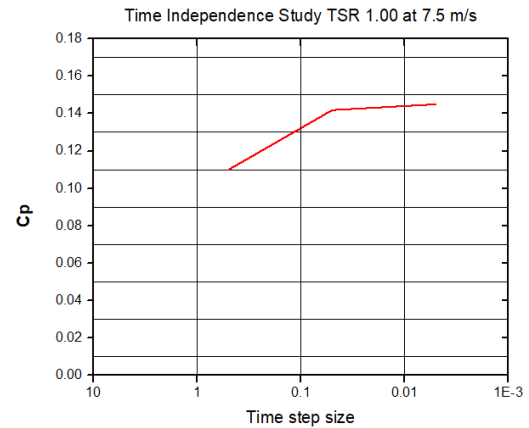


Figure 12. Time step independence study for hybrid VAWT.



Figure 13. C1 and C2 configurations of hybrid VAWT.

performance under varying wind conditions. Furthermore, the experimental results obtained from a meticulously crafted scaled-down model were also analyzed. These empirical findings serve as tangible validations of the computational predictions, facilitating a comprehensive assessment of the model's accuracy in replicating real-world phenomena. The analysis contributes to an enhanced understanding of the performance characteristics inherent to J-shaped hybrid VAWT configurations, thereby informing their potential suitability for wind energy utilization across diverse environmental scenarios.

4.1. VARIATION OF C_p WITH TSR FOR THREE J-SHAPED HYBRID VAWT CONFIGURATIONS

The main focus of the performance evaluation was based on the torque output and the associated power coefficient obtained for the hybrid VAWT model. The C_p versus TSR plot for the three configurations is shown in **Figure 14**. The graphical representation in the figure vividly illustrates a significant insight into the aerodynamic performance of the Hybrid VAWT under diverse configurations. Notably, the attained maximum power coefficient (C_p) of

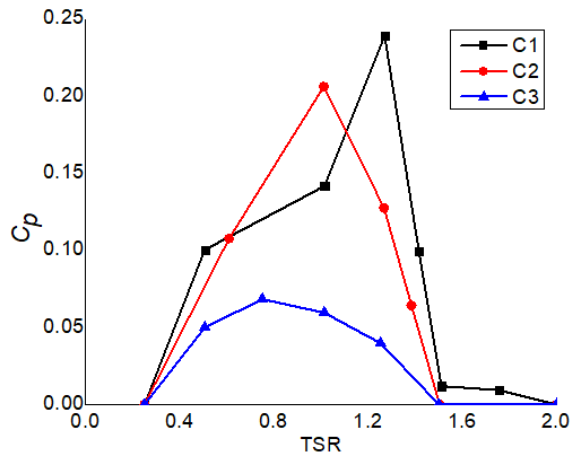


Figure 14. Cp versus TSR for three J-shaped configurations.

0.24 serves as a noteworthy highlight, particularly when juxtaposed against alternative designs. Of paramount importance is the observation that this peak Cp of 0.24 was realized at a TSR of 1.25. This specific TSR emerges as a distinct focal point, outshining the results obtained from other configurations. The implication of this finding cannot be understated, as it underscores the efficacy of the chosen design and the pronounced advantage it holds over alternative configurations at this particular operational range. The manifestation of this enhanced Cp at a TSR of 1.25 is indicative of the synergetic interaction between the J-shaped configuration and the turbine’s aerodynamics. The augmentation of power conversion efficiency at this specific TSR underscores the strategic potential of the J-shaped design, positioning it as a viable solution for maximizing energy extraction within the operational envelope of the hybrid VAWT. In comparison to the alternative configurations, the superior Cp performance at the critical TSR of 1.25 further solidifies the notion that the J-shaped configuration has been adeptly tailored to harmonize with the turbine’s characteristics. This achievement not only serves as a testament to the thoroughness of the study but also underscores the practical viability of the J-shaped design within the dynamic wind regime of the hybrid VAWT.

4.2. EXPERIMENTAL RESULTS OBTAINED FROM SCALED-DOWN MODEL

In a real-world scenario, maintaining a consistent incoming freestream velocity may restrict the range of

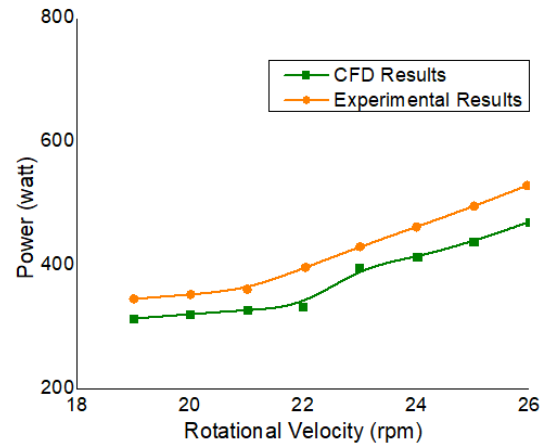


Figure 15. Comparison of experimental and numerical results for C2 configuration.

Table 15. Comparative analysis of CFD and experimental results

TSR	C_p (CFD)	C_p (Exp)	% Error
0.50	0.10	0.103	2.9
1.00	0.14	0.146	4.1
1.25	0.24	0.248	3.2
1.50	0.12	0.125	4.0
1.75	0.05	0.051	2.0
2.00	0.01	0.0105	4.8

available rotational velocity values. To modify rotational velocity, adjustments in the incoming freestream velocity must be made to introduce variations. The outcomes pertaining to the C2 configuration of the scaled-down model are visually presented in Figure 15. A noteworthy highlight of this investigation is the remarkable congruence observed between the experimental outcomes and the CFD simulations. The reliability of the CFD predictions is unmistakable, as indicated by a minimal disparity of less than 5% when compared to the experimental results. Furthermore, a comparative analysis of CFD and experimental results in terms of Cp versus TSR has also been presented in Table 15. The maximum percentage error was found to be 4.8%. This concordance between empirical observations and simulation outcomes highlights the accuracy and reliability of the applied CFD

methodology in capturing the complex aerodynamic interactions within the hybrid VAWT system. The investigation transcends the conventional symmetrical and cambered airfoils by introducing the innovative J-shaped configuration. The resulting impact on power coefficients was thoroughly examined across diverse TSR scenarios. This paper elucidates the intricate relationship between airfoil design modifications and turbine performance, shedding light on the potential for substantial efficiency enhancements in hybrid VAWT applications.

5. CONCLUSION

In this research endeavor, the exploration of a groundbreaking J-shaped configuration as an innovative airfoil design alternative, with a primary focus on augmenting the performance of Hybrid VAWTs, was meticulously conducted. The investigation yielded profound insights into the multifaceted effects of this design modification. Foremost, the incorporation of the J-shaped configuration emerged as a pivotal advancement in fortifying the self-starting capability of the turbine. This enhancement holds great promise for ensuring the reliable operation of the turbine, even in the face of fluctuating wind speeds. Beyond the critical starting phase, the study revealed a remarkable transformation in the power conversion efficiency of the turbine, exemplified by a notable peak power coefficient of 0.24 achieved at a TSR of 1.25. This translated into a peak power output of 526 watts, realized at a rotational speed of 26 RPM. Such notable advancements underscore the tangible impact of the J-shaped configuration on the turbine's energy conversion capabilities. The consequential increase in power output bears significant implications for bolstering the energy yield of Hybrid VAWTs in practical applications. Furthermore, the research ventured beyond the immediate effects of the J-shaped configuration by shedding light on its influence on the underlying symmetrical and cambered airfoil designs. This comprehensive approach not only accentuated the merits of the J-shaped but also emphasized its potential to reshape the performance characteristics of conventional airfoil profiles. In addition, a remarkable hallmark of this study was the outstanding alignment observed between experimental results and CFD simulations. The fidelity of the CFD predictions became evident in the negligible disparity of less than 5% when compared to the

experimental findings. Furthermore, a comparative analysis of CFD and experimental results in terms of C_p versus TSR has also been presented, with the maximum percentage error found to be 4.8%. This concordance between empirical observations and simulation outcomes highlights the accuracy and reliability of the applied CFD methodology in capturing the complex aerodynamic interactions within the hybrid VAWT system. In conclusion, this study underscores the remarkable potential of the J-shaped configuration as a transformative airfoil design for enhancing both the starting performance and energy conversion efficiency of Hybrid VAWTs. By providing a comprehensive understanding of the intricate interactions between design alterations and turbine performance, this research paves the way for more effective and sustainable wind energy solutions. The findings not only contribute to the advancement of hybrid VAWT technology but also stimulate further exploration and innovation within the renewable energy sector.

NOMENCLATURE & ABBREVIATIONS

VAWT	Vertical axis wind turbine
RPM	Revolutions per minute
HAWT	Horizontal axis wind turbine
CFD	Computational fluid dynamics
BOI	Body of influence
TSR	Tip speed ratio
C_L	Lift coefficient
C_D	Drag coefficient
C_T	Tangential force coefficient
C_N	Normal force coefficient
S_L	Scaling factor of length
S_V	Scaling factor of velocity
S_F	Scaling factor of aerodynamic force
S_P	Scaling factor of power
c	Chord length (m)
ρ	Fluid density (kg/m^3)
θ	Azimuth angle (deg)
V	Wind speed (m/s)

λ	TSR
A	Swept area (m ²)
C_p	Power coefficient
ω	Angular velocity (rad/s)
P	Output power (Watt)
W	Relative flow velocity
R	Rotor radius
α	Angle of attack (deg)
σ	Solidity
\vec{W}	Resultant velocity vector

DISCLOSURE STATEMENT

The authors declare no conflict of interest.

REFERENCES

- [1] Ahmad M, Shahzad A, Akram F, et al., 2022, Determination of Efficient Configurations of Vertical Axis Wind Turbine Using Design of Experiments. *Proceedings of the Institution of Mechanical Engineers, Part A: Journal of Power and Energy*, 236(8): 1558–1581.
- [2] Kavade RK, Ghanegaonkar PM, 2017, Design and Analysis of Vertical Axis Wind Turbine for Household Application. *Journal of Clean Energy Technologies*, 5(5): 353–358.
- [3] Roga S, Bardhan S, Kumar Y, et al., 2022, Recent Technology and Challenges of Wind Energy Generation: A Review. *Sustainable Energy Technologies and Assessments*, 52: 102239.
- [4] Msigwa G, Ighalo JO, Yap P-S, 2022, Considerations on Environmental, Economic, and Energy Impacts of Wind Energy Generation: Projections Towards Sustainability Initiatives. *Science of The Total Environment*, 849: 157755.
- [5] Rafiei B, Gharali K, Soltani M, 2023, Optimized Configuration with Economic Evaluation for Shrouded Vertical Axis Wind Turbines Applicable for Urban Structures. *Energy Science & Engineering*, 11(10): 3699–3720.
- [6] Linnerud K, Dugstad A, Rygg BJ, 2022, Do People Prefer Offshore to Onshore Wind Energy? The Role of Ownership and Intended Use. *Renewable and Sustainable Energy Reviews*, 168: 112732.
- [7] Yang B, Liu B, Zhou H, et al., 2022, A Critical Survey of Technologies of Large Offshore Wind Farm Integration: Summary, Advances, and Perspectives. *Protection and Control of Modern Power Systems*, 7(1): 17.
- [8] Ahmad M, Shahzad A, Shah SIA, 2023, Experimental Investigation and Analysis of Proposed Hybrid Vertical Axis Wind Turbine Design. *Energy & Environment*. <https://doi.org/10.1177/0958305X231181675>
- [9] Olczak P, Surma T, 2023, Energy Productivity Potential of Offshore Wind in Poland and Cooperation with Onshore Wind Farm. *Applied Sciences*, 13(7): 4258.
- [10] López-Queija J, Robles E, Jugo J, et al., 2022, Review of Control Technologies for Floating Offshore Wind Turbines. *Renewable and Sustainable Energy Reviews*, 167: 112787.
- [11] Zhou Q, Wang S, Liu J, et al., 2022, Geological Evolution of Offshore Pollution and Its Long-Term Potential Impacts on Marine Ecosystems. *Geoscience Frontiers*, 13(5): 101427.
- [12] Ahmad M, Rehman I, 2023, Investigating Aerodynamic Performance of Vertical Axis Wind Turbines Using Computational Techniques. *Journal of Power Generation Technology*, 1(1): 20–41.
- [13] Cao L, Ge M, Gao X, et al., 2022, Wind Farm Layout Optimization to Minimize the Wake Induced Turbulence Effect on Wind Turbines. *Applied Energy*, 323: 119599.
- [14] Buharia M, Ahmad A, Isa MM, 2020, Comparative Analysis Between Hybrid and Conventional Vertical Axis Wind Turbines Performances. *Premier Journal of Engineering and Applied Sciences*, 1(3): 1119.015.
- [15] Tjiu W, Marnoto T, Mat S, et al., 2015, Darrieus Vertical Axis Wind Turbine for Power Generation I: Assessment of Darrieus VAWT Configurations. *Renewable energy*, 75: 50–67.
- [16] Ragheb M, 2008, Vertical Axis Wind Turbines, viewed March 26, 2023, <https://www.scribd.com/doc/101544049/Vertical-Axis-Wind-Turbines>
- [17] Venkatraman K, Moreau S, Christophe J, et al., 2023, Numerical Investigation of H-Darrieus Wind Turbine Aerodynamics at Different Tip Speed Ratios. *International Journal of Numerical Methods for Heat & Fluid Flow*, 33(4): 1489–1512.
- [18] Mohamed M, Ali A, Hafiz A, 2015, CFD Analysis for H-Rotor Darrieus Turbine as a Low Speed Wind Energy Converter. *Engineering Science and Technology*, 18(1): 1–13.
- [19] Burton T, Jenkins N, Sharpe D, et al., 2011, *Wind Energy Handbook*. John Wiley & Sons, New Jersey.
- [20] Alsabri A, Oreijah M, Mohamed MH, 2019, A Comparison Study of Aerofoils Used in H-Rotor Darrieus Wind Turbine. *International Journal of Science and Engineering Investigations*, 8(90): 22–28.
- [21] Akwa JV, Vielmo HA, Petry AP, 2012, A Review on the

- Performance of Savonius Wind Turbines. *Renewable and Sustainable Energy Reviews*, 16(5): 3054–3064.
- [22] Bausas MD, Danao LAM, 2015, The Aerodynamics of a Camber-Bladed Vertical Axis Wind Turbine in Unsteady Wind. *Energy*, 93: 1155–1164.
- [23] Tartuferi M, D'Alessandro V, Montelpare S, et al., 2015, Enhancement of Savonius Wind Rotor Aerodynamic Performance: A Computational Study of New Blade Shapes and Curtain Systems. *Energy*, 79: 371–384.
- [24] Ahmad M, Shahzad A, Akram F, et al., 2022, Design Optimization of Double-Darrieus Hybrid Vertical Axis Wind Turbine. *Ocean Engineering*, 254: 111171.
- [25] Subramanian A, Yogesh SA, Sivanandan H, et al., 2017, Effect of Airfoil and Solidity on Performance of Small Scale Vertical Axis Wind Turbine Using Three Dimensional CFD Model. *Energy*, 133: 179–190.
- [26] Talukdar PK, Kulkarni V, Chatterjee D, et al., 2023, Vertical-Axis Hybrid Turbines as Wind and Hydrokinetic Energy Harvesters: Technological Growth and Future Design Strategies. *Sādhanā*, 48(3): 178.
- [27] Altmimi AI, Alaskari M, Abdullah OI, et al., 2021, Design and Optimization of Vertical Axis Wind Turbines Using QBlade. *Applied System Innovation*, 4(4): 74.
- [28] Elsakka MM, Ingham DB, Ma L, et al., 2022, Response Surface Optimisation of Vertical Axis Wind Turbine at Low Wind Speeds. *Energy Reports*, 8: 10868–10880.
- [29] Ahmad M, Shahzad A, Qadri MNM, 2022, An Overview of Aerodynamic Performance Analysis of Vertical Axis Wind Turbines. *Energy & Environment*, 34(7): 2815–2857.
- [30] Tripathi A, Das P, Aggarwal T, et al., 2022, Efficiency Enhancement of a Hybrid Vertical Axis Wind Turbine by Utilizing Optimum Parameters. *Materials Today: Proceedings*, 62(Part 6): 3582–3588.
- [31] Cai X, Zhang Y, Ding W, et al., 2019, The Aerodynamic Performance of H-Type Darrieus VAWT Rotor With and Without Winglets: CFD Simulations. *Energy Sources, Part A: Recovery, Utilization, and Environmental Effects*. <https://doi.org/10.1080/15567036.2019.1691286>
- [32] Mohamed MH, 2012, Performance Investigation of H-Rotor Darrieus Turbine with New Airfoil Shapes. *Energy*, 47(1): 522–530.
- [33] Lositaño ICM, Danao LAM, 2019, Steady Wind Performance of a 5 kW Three-Bladed H-Rotor Darrieus Vertical Axis Wind Turbine (VAWT) with Cambered Tubercle Leading Edge (TLE) Blades. *Energy*, 175: 278–291.
- [34] Zamani M, Maghrebi MJ, Varedi SR, 2016, Starting Torque Improvement Using J-Shaped Straight-Bladed Darrieus Vertical Axis Wind Turbine by Means of Numerical Simulation. *Renewable Energy*, 95: 109–126.
- [35] Loganathan B, Zaid M, Chowdhury H, 2022, Harvesting Wind Energy from the Complex Urban Environment Using CFD Approach. *AIP Conference Proceedings*, 2681(1): 020099.
- [36] Shao Y, Su J, Tu Y, et al., 2023, Assessment of the Aerodynamic Benefits of Collocating Horizontal and Vertical-Axis Wind Turbines in Tandem Using Actuator Line Model. *Physics of Fluids*, 35(7): 075115.
- [37] Khan AA, Ahmad M, Ashraf M, 2016, Residual Life Estimation of an Attach Angle for a Cargo Aircraft. *Journal of Failure Analysis and Prevention*, 16: 1126–1133.
- [38] Belabes B, Paraschivoiu M, 2022, Proceedings of the Canadian Society for Mechanical Engineering International Congress 2022, June 5–8, 2022: CFD Study of the Aerodynamic Performance of a Vertical Axis Wind Turbine in the Wake of Another Turbine. *CSME, Alberta*.
- [39] Saeed RI, Al-Manea A, Ibrahim AK, 2022, Numerical Investigation on the Effect of Profile and Blade Numbers in a Savonius Vertical Axis Wind Turbine. *CFD Letters*, 14(9): 75–88.
- [40] Ngoc DM, Luengchavanon M, Anh PT, et al., 2022, Shades of Green: Life Cycle Assessment of a Novel Small-Scale Vertical Axis Wind Turbine Tree. *Energies*, 15(20): 7530.
- [41] Alaimo A, Esposito A, Messineo A, et al., 2015, 3D CFD Analysis of a Vertical Axis Wind Turbine. *Energies*, 8(4): 3013–3033.
- [42] Zamani M, Nazari S, Moshizi SA, et al., 2016, Three Dimensional Simulation of J-Shaped Darrieus Vertical Axis Wind Turbine. *Energy*, 116: 1243–1255.
- [43] Ahmad M, Zafar MH, 2023, Enhancing Vertical Axis Wind Turbine Efficiency Through Leading Edge Tubercles: A Multifaceted Analysis. *Ocean Engineering*, 288: 116026.
- [44] Hosseini A, Goudarzi N, 2019, Design and CFD Study of a Hybrid Vertical-Axis Wind Turbine by Employing a Combined Bach-Type and H-Darrieus Rotor Systems. *Energy Conversion and Management*, 189: 49–59.
- [45] Bhuyan S, Biswas A, 2014, Investigations on Self-Starting and Performance Characteristics of Simple H and Hybrid H-Savonius Vertical Axis Wind Rotors. *Energy Conversion and Management*, 87: 859–867.
- [46] Benmoussa A, Páscoa JC, 2023, Enhancement of a Cycloidal Self-Pitch Vertical Axis Wind Turbine Performance Through DBD Plasma Actuators at Low Tip Speed Ratio. *International Journal of Thermofluids*, 17: 100258.
- [47] Dol SS, Khamis A, Abdallftah MT, et al., 2022, CFD Analysis of Vertical Axis Wind Turbine with Winglets. *Renewable Energy Research and Applications*, 3(1): 51–59.

- [48] Ahmad M, Hussain ZL, Shah SIA, et al., 2021, Estimation of Stability Parameters for Wide Body Aircraft Using Computational Techniques. *Applied Sciences*, 11(5): 2087.
- [49] Howell R, Qin N, Edwards J, et al., 2010, Wind Tunnel and Numerical Study of a Small Vertical Axis Wind Turbine. *Renewable Energy*, 35(2): 412–422.
- [50] Balduzzi F, Bianchini A, Ferrara G, et al., 2016, Dimensionless Numbers for the Assessment of Mesh and Timestep Requirements in CFD Simulations of Darrieus Wind Turbines. *Energy*, 97: 246–261.
- [51] Satrio D, Utama IKAP, Mukhtasor M, 2018, The Influence of Time Step Setting on the CFD Simulation Result of Vertical Axis Tidal Current Turbine. *Journal of Mechanical Engineering and Sciences*, 12(1): 3399–3409.



Muhammad Ahmad holds a Master's degree in Aerospace Engineering and specializes in Computational Fluid Dynamics (CFD), Renewable Energy, Aerodynamics, Design Optimization, Fluid Mechanics, and Wind Energy Harvesting. With an academic background and expertise in these areas, he has contributed significantly to research and development efforts in the aerospace and renewable energy sectors. His passion for advancing aerospace engineering and wind energy technologies drives him to address complex challenges and strive for sustainable and efficient solutions.



Muhammad Zubair Abid holds a Bachelor's degree in aerospace engineering and is currently pursuing a Master's degree in Artificial Intelligence. With a keen interest in both aerospace and cutting-edge technology, he has embarked on a journey to merge his expertise in engineering with the rapidly evolving field of AI. Throughout his academic career, Zubair has demonstrated a strong aptitude for learning and problem-solving. He is deeply passionate about exploring the intersection of aerospace and AI, seeking to leverage his background in engineering to tackle complex challenges in artificial intelligence.

Publisher's note

Art and Design Publishing remains neutral with regard to jurisdictional claims in published maps and institutional affiliations.